JASMAC
Conference of the Japan Society of Microgravity Application

P07

Numerical simulation of thermal-solutal Marangoni convection in a shallow rectangular cavity with the effect of radiative heat transfer under zero gravity

Jiangao ZHANG, Yasunori OKANO

Department of Materials Engineering Science, Osaka University

1. Introduction

Marangoni flow has been widely concerned for its rich dynamical features and its wide existence in nature and industrial processes, such as oceanography [1)], droplet [2)], painting [3)] and crystal growth [4)]. To the best of our knowledge, most studies considering Marangoni convection adopted an assumption of unrealistic adiabatic free surface. the consideration of interfacial heat transfer on the free surface is necessary for accurate predictions and has a significant effect on the quality of final products, especially in welding and crystal growth. Therefore, in this work, we performed a series of three-dimensional numerical simulations considering the effect of radiative heat transfer on thermal-solutal Marangoni convection in a shallow rectangular cavity with mutually perpendicular thermal and concentration gradients, with the aim of shedding further light on the related flow characteristics and flow pattern transitions in the cavity.

2. Numerical method

The fluid motion in a three-dimensional rectangular cavity with a free surface at the top boundary as shown in **Fig. 1** is considered in the Cartesian coordinate system. A high and low temperature values, T_h and T_l, are set at the left and right boundaries, and the concentration values of C_h and C_l are prescribed at the back and front boundaries. Marangoni convection along the free surface is driven by the surface tension gradient due to a temperature gradient in x and concentration gradient in y. Meanwhile, radiation is considered on the free surface, and T_a is the ambient temperature.

For simplification, we assume that (i) the free surface does not deform; (ii) the fluid is incompressible and Newtonian, and its physical properties do not depend on temperature and concentration except for surface tension; (iii) the no-slip boundary condition is applied except for the top free surface.

By using L, L^2/ν, ν/L as the characteristic length, time, velocity, respectively, the dimensionless governing equations are the conservation of mass, momentum, energy, and mass transfer:

$$\nabla \cdot V = 0 \tag{1}$$

$$\frac{\partial V}{\partial \tau} + V \cdot \nabla V = -\nabla P + \nabla^2 V \tag{2}$$

$$\frac{\partial \Theta}{\partial \tau} + V \cdot \nabla \Theta = -\frac{1}{Pr}\nabla^2 \Theta \tag{3}$$

$$\frac{\partial \Phi}{\partial \tau} + V \cdot \nabla \Phi = -\frac{1}{Sc} \nabla^2 \Phi \tag{4}$$

where ν is the kinematic viscosity, the nondimesional temperature and concentrations are defined as $\Theta = (T - T_l)/(T_h - T_l)$ and $\Phi = (C - C_l)/(C_h - C_l)$, τ and P are the dimensionless time and pressure. $Pr = \nu/\alpha$ is the Prandtl number, and $Sc = \nu/D$ is the Schmidt number, where α and D are the thermal diffusivity and the diffusion coefficient of the fluid ($Pr = 0.01$, $Sc = 1$), respectively.

No-slip boundary condition is applied except for top surface, and the boundary condition along free surface are follows:

$$\frac{\partial V_x}{\partial z} = -Ma_{\mathrm{T}} \frac{\partial \Theta}{\partial x} - Ma_{\mathrm{C}} \frac{\partial \Phi}{\partial x} \tag{4}$$

$$\frac{\partial V_y}{\partial z} = -Ma_{\mathrm{T}} \frac{\partial \Theta}{\partial y} - Ma_{\mathrm{C}} \frac{\partial \Phi}{\partial y} \tag{5}$$

$$V_z = 0 \tag{6}$$

$$\frac{\partial \Theta}{\partial z} = -R_{\mathrm{ad}} (\Theta - \Theta_{\mathrm{a}}) = Q_r, \quad \frac{\partial \Phi}{\partial z} = 0 \tag{7}$$

where Q_r is the heat flux on the whole free surface, $\Theta_a = (T_a - T_l)/(T_h - T_l)$ is the dimensionless ambient temperature. $R_{ad} = \varepsilon\sigma_{SB}(T^2+T_a^2)(T-T_a)/k$ is the radiation number, where ε, σ_{SB} and k are respectively the emissivity, Stefan-Boltzmann constant and thermal conductivity.

The thermal and solutal Marangoni numbers are defined as

$$Ma_{\mathrm{T}} = -\sigma_{\mathrm{T}} \frac{(T_{\mathrm{h}} - T_{\mathrm{l}})L}{\mu \nu}, \quad Ma_{\mathrm{C}} = \sigma_{\mathrm{C}} \frac{(C_{\mathrm{h}} - C_{\mathrm{l}})L}{\mu \nu} \tag{8}$$

where $\sigma_T = \partial\sigma/\partial T$ (<0) and $\sigma_C = \partial\sigma/\partial C$ (>0) are the surface tension coefficients of the temperature and concentration fields, respectively. The directions of Marangoni flows are shown in **Fig. 1**. In addition, the overall contributions of thermal and solutal Marangoni flows are in the same order for all the cases considered, the Marangoni ratio $Ma_\sigma = Ma_C/Ma_T = 1$.

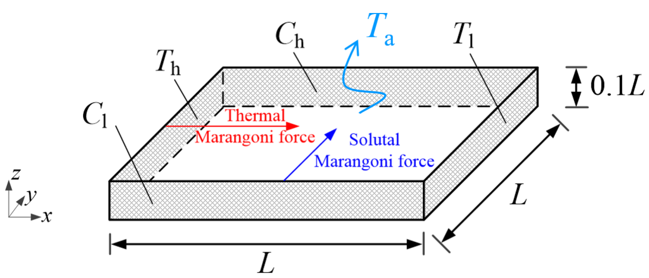

Fig. 1 Numerical computational domain and the boundary conditions. The arrows indicate the directions of each Marangoni convections.

The finite volume method with nonuniform grid is applied to discretize the governing equations and boundary conditions, which are solved by the pressure-implicit split-operator (PISO) algorithm in OpenFOAM. Details of the implementation of the numerical procedure can be found in the work of Minakuchi *et al.* [5]. In addition, the numerical method is validated in our previous work [6] and the mesh dependency is evaluated.

3. Results and discussion

3.1 Basic flow and stability

When Ma_T is relatively small, the Marangoni convection is the steady flow, which is called as the basic flow. **Figure 2** shows the distributions of temperature gradient gradΘ_x and velocity V_x along the AB line (y = 0.5) at various free surface conditions. It is obvious that radiative heat transfer has a significant influence on the temperature and velocity fields. With the increase of ambient temperature, the overall radiative heat transfer on the free surface exhibits transition from heat loss to heat gain. Thus, as depicted in **Fig. 2(a)**, the maximum temperature gradient first decreases then increases, and the position of that changes from left to right sidewalls. It is noted that, at Θ_a = 0.5 (green line), although the temperature gradient close to sidewalls is larger than that of the adiabatic case (orange line), it is contrary at the central region, while the temperature gradient is always approximately -1 under the adiabatic condition. Therefore, the similar distributions of streamline, temperature, and concentration overall are observed at the adiabatic case. In addition, as shown in **Fig. 2(b)**, the distribution of lateral velocity also changes accordingly, which greatly affects the flow structure.

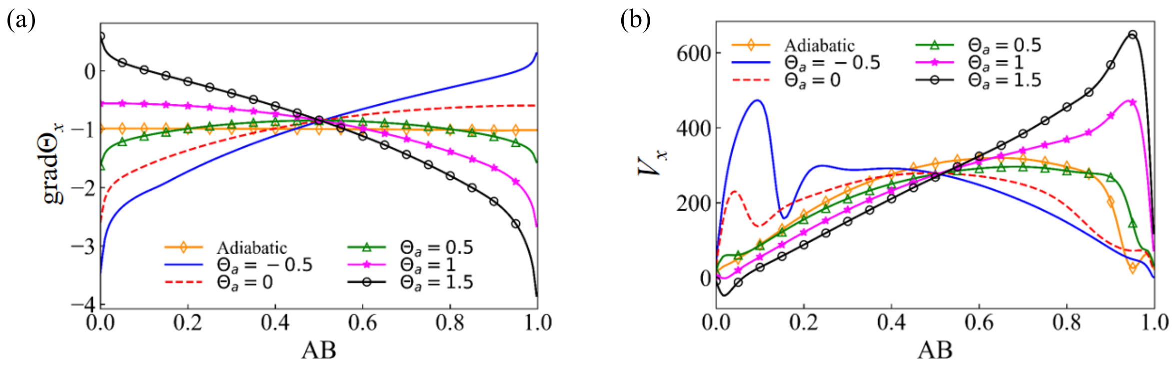

Fig. 2 Distributions of temperature gradient gradΦ_x (a) and velocity V_x (b) along AB line (y=0.5) on the free surface at Ma_T = 1.5 ×10^4.

3.2 Oscillatory flow

When the thermal Marangoni number exceeds a critical value, the thermal-solutal Marangoni flow bifurcates to an oscillatory flow. **Figure 3** shows the time dependencies of the longitudinal velocity V_y, temperature Θ and concentration Φ at different sampling points at Ma_T = 4 ×10^4 at different free surface conditions. The sampling points (M, N, P) are respectively located at (x, y, z) = (0.1, 0.5, 0.1), (x, y, z) = (0.8, 0.8, 0.1) and (x, y, z) = (0.5, 0.5, 0.1) on the free surface. It can be found from **Fig. 3** that there is a fixed phase difference between temperature, concentration and velocity oscillations. The phase lag phenomena is the basic characteristic of flow instabilities and results in the occurrence of hydrothermal wave (HTW) and hydrosolutal wave (HSW) on the free surface. Similar observations have been reported not only in pure Marangoni flow [7)] but also in thermal-solutal Marangoni flow [8)] with an assumption of adiabatic free surface.

The coupling effect of the thermal-solutal Marangoni flow and the radiative heat transfer has a significant influence on the phase lag. At Θ_a = -0.5, the thermal Marangoni effect is dominant near point M due to the high temperature gradient, while the solutal Marangoni effect is dominant near point N. This relative contribution of thermal and solutal Marangoni flows would result in the change of phase lag difference among those oscillations, as shown in **Fig. 3 (a)- 3(c)**. In addition, the sequence of phase lag among the temperature, concentration oscillations depends on radiative heat transfer, as demonstrated in **Fig. 3 (b)** and **3 (d)**, while the velocity oscillation always lags the others.

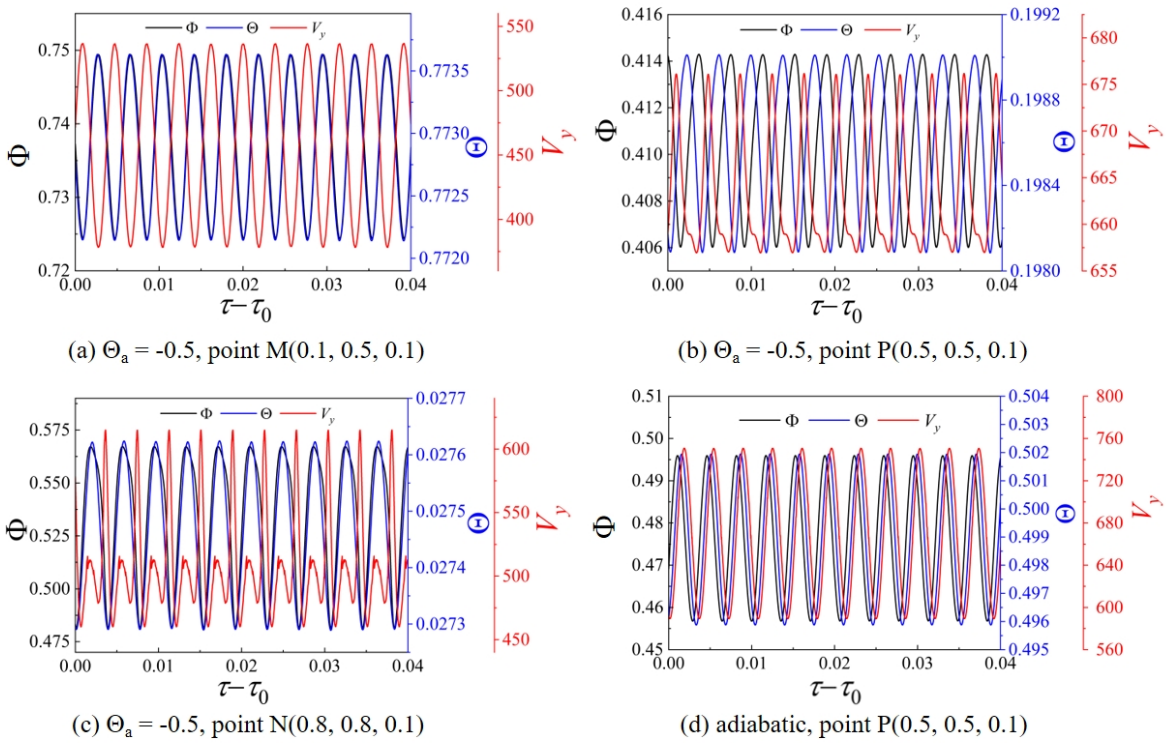

Fig. 3 Time variation of the longitudinal velocity V_y, temperature Θ and concentration Φ at different sampling points at $Ma_T = 4 \times 10^4$ for different free surface conditions.

4. Conclusion

A series of three-dimensional simulations under the effect of radiative heat transfer gradients have been investigated on the thermal-solutal Marangoni convection in a rectangular cavity that is subjected to mutually perpendicular temperature and concentration, and the following conclusions are obtained:

(1) With the increase of ambient temperature, the maximum temperature gradient first decreases then increases, and the positions of that transit from left to right sidewalls, which in turn greatly affects the concentration and velocity fields in the whole system.

(2) Once the flow destabilizes, the fluctuations of temperature and concentration would appear in the forms of hydrothermal wave and hydrosolutal wave on the free surface. In addition, the coupling effect of the thermal-solutal Marangoni flow and the radiative heat transfer has a significant influence on the phase lag phenomena.

Acknowledgements

This work was partially supported by JSPS KAKENHI, Grant No. JP19K22015. The computational resources were provided by the Research Institute for Information Technology, Kyushu University, Japan, and Collaborative Research Program for Young Women Scientists provided by Academic Center for Computing and Media Studies, Kyoto University, Japan, and Initiative on Promotion of Supercomputing for Young or Women Researchers provided by Information Technology Center, Tokyo University, Japan.

References

1) D. Walker and S. DeLong: Contrib. Mineral. and Petrol., **79** (1982) 231.

2) M. Schmitt and H. Stark: Phys. Fluids, **28** (2016) 012106.

3) J.-G. Zhang, Y. Okano and S. Dost: Int. J. Heat Mass Transfer, **178** (2021) 121578.

4) T. Yano and K. Nishino: Adv. Space Res., **66** (2020) 2047.

5) H. Minakuchi, Y. Takagi, Y. Okano, K. Mizoguchi, S. Gima and S. Dost: J. Adv. Res. Phys., **3** (2012) 011201.

6) J.-G. Zhang, A. Sekimoto, Y. Okano and S. Dost: Phys. Fluids, **32**, (2020) 102108.

7) M. K. Smith: Phys. Fluids, **29** (1986) 3182.

8) J.-J. Yu, Y.-R. Li, J.-C. Chen, Y. Zhang and C.-M. Wu: Int. J. Heat Mass Transfer, **113** (2017) 40.a